Reactions of Polycyclic Aromatic Hydrocarbon Radical Cations with Model Biological Nucleophiles

Andy B. Whitehill and M. George
University of Nebraska-Lincoln, Department of Chemistry, Lincoln, Nebraska, USA

Michael L. Gross
Washington University, Department of Chemistry, St. Louis, Missouri, USA

The determination of gas-phase reactivity of a series of polycyclic aromatic hydrocarbons (PAHs) with nucleophiles is directed at achieving isomer differentiation through ion-molecule reactions and collisionally activated decomposition spectra. A series of PAH isomers form gas-phase $[\text{adduct} - \text{H}]^+$ ions with the reagent nucleophiles pyridine and N-methylimidazole. Collisionally activated decomposition spectra of the $[\text{adduct} - \text{H}]^+$ ions of the pyridine/PAH systems are dominated by products formed by losses of C_5H_4N, C_5H_5N (presumably neutral pyridine), and C_5H_6N. Collisional activation of PAH/N-methylimidazole $[\text{adduct} - \text{H}]^+$ ions causes analogous losses of $C_4H_5N_2$, $C_4H_6N_2$ (presumably neutral N-methylimidazole), and $C_4H_7N_2$. The relative abundances of the ions that result from these losses are highly isomer specific for N-methylimidazole but less so for pyridine. Furthermore, PAH/N-methylimidazole $[\text{adduct} - \text{H}]^+$ ions undergo a series of metastable-ion decompositions that also provide highly isomer-specific information. The $C_4H_7N_2$ (from PAH/N-methylimidazole product ions) and C_5H_6N (from PAH/pyridine product ions) losses tend to increase with the ΔH_f of the PAH radical cation. In addition, it is shown that the fragmentation patterns of these gas-phase PAH/nucleophile adducts are similar to fragmentation patterns of PAH/nucleoside adducts generated in solution, which suggests that the structures of products formed in gas-phase reactions are similar to those produced in solution. (*J Am Soc Mass Spectrom* 1996, 7, 628–638)

Polycyclic aromatic hydrocarbons (PAHs) have been known to be carcinogenic since the early 1900s. Because they are mutagenic and ubiquitous in the environment, the need to detect and identify PAHs has continued to be an analytical challenge. Separation procedures and detection methods continue to be developed so that smaller and more complex samples can be analyzed and isomeric PAHs can be distinguished.

Gas chromatography (GC) and packed column GC coupled with UV absorption or fluorescence detection account for most of the methods for PAH determination through the 1960s and early 1970s [1]. Books by Bjorseth [2], Lee [3], and Vo-Dinh [4] and the articles in reference 1 provide reviews of the history of PAH determination by GC and other methods.

The low volatility of some PAHs and their occurrence as complex mixtures provide the driving force for the development of analysis techniques. High-performance liquid chromatography (HPLC) [2–5], mi-cellar chromatography [4, 6], capillary electrophoresis [7], and supercritical fluid extraction [4, 8] all have been successfully applied to PAH separation and determination.

Mass spectrometry has played an important role in the determination of PAHs. In early applications, mass spectrometers were employed as detectors after GC or HPLC separations [2–4]. For example, Wise et al. [9] demonstrated the analysis of reference air-particulate samples with liquid chromatography and GC separation followed by electron ionization–mass spectrometry analysis. Another approach is GC with pulsed-photon ionization and time-of-flight (TOF) mass spectrometry, for the analysis of coeluting PAH isomers [10].

The most effective and often used mass spectrometric techniques for the determination of PAHs, including the differentiation of PAH isomers, are electron ionization (EI) and chemical ionization (CI) with quadrupole and magnetic sector mass spectrometers. PAH determination also was shown to be possible with matrix-assisted laser desorption ionization–TOF [11] and ion mobility spectrometry [12].

Isomeric PAHs are known to isomerize through

Address reprint requests to Dr. Michael L. Gross, Washington University, Department of Chemistry, 1 Brookings Drive, St. Louis, MO 63130.

extensive rearrangements to produce common intermediates that give identical losses upon high-energy ionization or collisional activation (CA). As a result, EI and collisionally activated dissociation (CAD) spectra of PAH isomers are usually indistinguishable. To remedy this problem, Shushan and Boyd [13] and Shushan et al. [14] demonstrated isomeric differentiation of PAHs with metastable-ion analysis. These lower-energy ions give spectra more indicative of the neutral precursor than do the more energized ions formed by high-energy EI or CA.

Cooks and co-workers [15] studied gas-phase PAH ions with a variety of techniques. They showed that PAH ions abstract methyl, ethyl, and propyl groups under ion-surface reaction conditions, and that surface-induced dissociation spectra of PAHs vary with collision energy. They also showed that with molecular secondary-ion mass spectrometry, PAHs that contain a "bay region" yield larger [PAH + Ag]$^+$:M$^{+\cdot}$ ion abundance ratios than PAHs without a "bay region." More recently, they determined electron affinities of several PAHs by the kinetic method [16]. Gross and co-workers [17] showed that PAH ions that are formed by EI, CI, desorption, and photoionization methods and then fragmented by low- and high-energy collisional activation as singly and multiply charged ions, provide valuable information in understanding PAH gas-phase ion processes. The difficulty of PAH isomer differentiation was shown to be related to high internal energy capacity of these ions as reflected by the large dissociation energies, which allowed for ring opening and isomerization, and that resulted in the ultimate production of common fragments.

The most effective mass spectrometric technique for the differentiation of PAH isomers has been chemical ionization–mass spectrometry in which PAH neutrals are ionized by protonation or charge exchange [19–23]. Once created, the PAH ions can be compared or reacted with a common neutral. A detailed study on the gas-phase reactivity of pyrene showed that its radical cation is unreactive, whereas the [M – H]$^+$ aryl ions participate in cycloadditions and alkyl-halide addition reactions [18]. The lack of reactivity of the radical cation with the neutrals studied was attributed to the π-delocalization of charge and radical sites over the aromatic system.

Simonsick and Hites [19] used an argon/methane reagent gas mixture to create M$^+$ and [M + H]$^+$ PAH ions. The ratio of [M + H]$^+$ ion abundance to that of the radical cation (M$^{+\cdot}$), GC elution times, and ionization energies were used in the analysis of standard references and carbon-black samples. Although troubled by coeluting isomers, the technique is shown to be effective in the analysis of complex samples and in the differentiation of isomers. Recently, Burrows [20] demonstrated the formation of adducts for a series of PAHs reacting with dimethyl ether. In most cases, the relative amount of adduct ions depends on the nature of the PAH isomer.

Buchanan et al. [21] approached PAH isomer differentiation with a variety of methods. They showed that electron-capture negative ion CI is useful for PAH determination because there are significant differences in electron affinity. Furthermore, the authors showed that CI reactions with oxygen can be used to differentiate certain isomeric PAHs. Reactions of PAHs with dimethyl ether [22] under hydroxylation conditions [23] do produce products, but the information is limited for isomer differentiation.

This article describes a study of PAH isomer differentiation by means of CI in which reactions of PAH radical cations with neutral pyridine or N-methylimidazole are used to produce adducts. Isomer differentiation is achieved by comparing CAD and metastable-ion spectra of the gas-phase adducts of isomeric PAHs. The choice of neutral reagents is motivated by the work of Cavalieri and co-workers [25, 26, 28], who proposed that PAH radical cations, which are formed in biological systems through enzymatic one-electron oxidation or their decomposition products form PAH-DNA adducts [24]. PAH radical cations, formed both electrochemically and enzymatically, do give adduct formation in reactions with nucleosides [25]. Most adductions occur on the imidazole portion of·the purine bases adenine and guanine. In these and other studies, mass spectrometry was shown to be effective in the identification of PAH–nucleoside adduct structures [26]. We also showed in a preliminary study [27] that in an ionized mixture of pyridine and benzo[a]pyrene, an ion–molecule reaction product forms, but the adduct was not characterized. In addition, 7,12-dimethylbenz[a]anthracene/pyridine adducts also were shown to give structure-specific CAD spectra by using fast-atom bombardment for desorption and tandem mass spectrometry for analysis [28]. These studies suggest that neutral pyridine and N-methlyimidazole may be suitable derivatizing reagents for PAH radical cations.

The results presented here and in previously reported work on the reactions of benzene, naphthalene, and PAHs of higher mass serve as first steps in a program to establish whether there is a correlation between the gas-phase reactivity of PAHs and their biological activity [29]. A similar approach was taken by Freeman et al. [30] to determine whether the gas-phase reactions of allyl reagents and pyridine can be used to screen complex environmental samples for biologically active compounds.

Experimental

Materials

Anthracene, tetracene (2,3-benzanthracene), benz[a] anthracene (1,2-benzanthracene), benzo[a]pyrene, benzo-[e]pyrene, and N-methylimidazole were purchased from Sigma Chemical Co. (St. Louis, MO). Perylene,

1,2:5,6-dibenzanthracene, 1,2:3,4-dibenzanthracene, and pyridine were purchased from Aldrich Chemical Co. (Milwaukee, WI), and phenanthrene was purchased from J. T. Baker Chemical Co. (Phillipsburg, NJ). All chemicals were used as received.

Mass Spectrometry

Most experiments were carried out with a prototype VG ZAB-T four-sector mass spectrometer (VG Analytical Ltd., Manchester, UK) of BEBE design operated with a DEC 3000 Alpha 200 station with OPUS version 3.2 and a SIOS I interface. All ions were accelerated with a potential of +8 kV, and the mass resolving power was approximately 1500 (10% valley definition).

EI experiments were carried out with a VG EI/CI source, and ions were created with a filament current of 50 μA at 70 eV. CI experiments were performed with the same source (with the CI slit in place) operated at an ionization energy of 180 eV, emission current of 0.2 mA, and at a source-housing pressure of approximately 8×10^{-5} torr. The source was heated to 150 °C. Solid samples of the PAHs were admitted via a heated-solids probe, and the liquids pyridine and N-methylimidazole were admitted via a heated inlet reservoir. The probe temperature for each PAH was adjusted to optimize adduct ion abundance.

Reaction-chamber pressures in the chemical ionization source were measured with a custom-built pressure probe equipped with a thermocouple gauge. Pressures were not corrected for differences in thermal conductivity between air and the reactants because relative responses were not known.
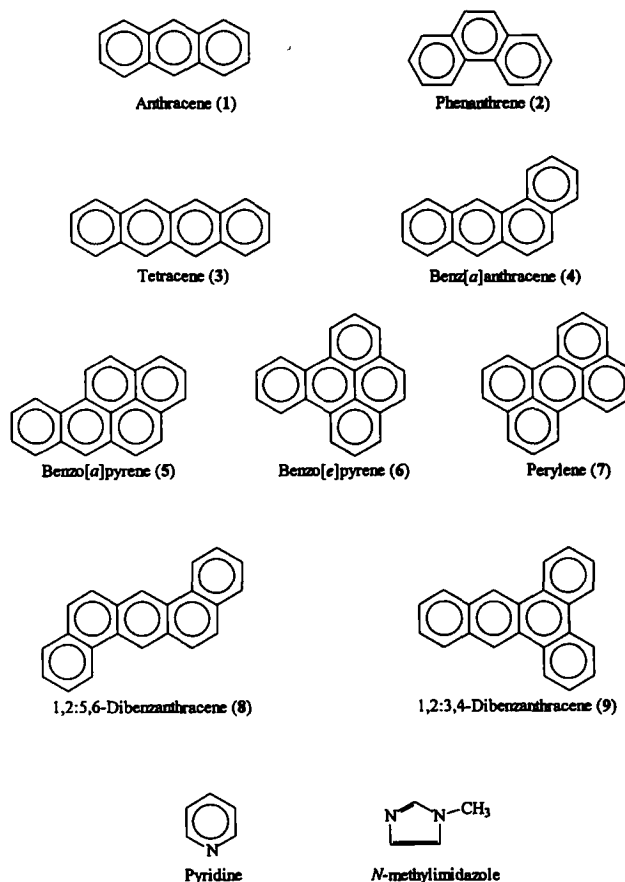
Metastable-ion decomposition spectra of the PAH radical cations were collected by focusing the precursor ion through MS1 (B_1E_1) and by using linked B_2E_2 scans for fragment ion detection. CAD spectra were collected in the same manner except dissociations were induced in a collision cell with helium at a pressure sufficient to attenuate the parent-ion beam by 50%. In both metastable-ion and CA analysis, the collision cell in the third field-free region (between MS1 and MS2) was floated at 4 kV to give a laboratory collision energy of 4 keV. Spectra were recorded by using the single-point detector.

Metastable-ion spectra of [adduct − H]$^+$ ions were collected with a Kratos Analytical (Ramsey, NJ) MS50 triple analyzer of EBE design [31]. Parent ions were focused to an evacuated collision cell with MS1 (E_1B) and the metastable decompositions were recorded with E_2. Metastable-ion decompositions of the [adduct − H]$^+$ ions were recorded with this instrument because the reproducibility of spectra was better when low-abundance fragment ions were recorded and because the ability to differentiate PAH isomers was better when relative abundances of metastable ions were compared.

Results and Discussion

Mass Spectrometry of PAH Radical Cations

The purpose of the research is to test whether the inherent gas-phase reactivity of a series of isomeric PAHs with models for purine bases permits isomeric PAHs to be distinguished. The compounds that were investigated are given as structures 1–9.

Anthracene (1)

Phenanthrene (2)

Tetracene (3)

Benz[a]anthracene (4)

Benzo[a]pyrene (5)

Benzo[e]pyrene (6)

Perylene (7)

1,2:5,6-Dibenzanthracene (8)

1,2:3,4-Dibenzanthracene (9)

Pyridine

N-methylimidazole

Although the bimolecular reactivity of the PAHs is the principal theme, we felt it was important to study first the fragmentation chemistry of these molecules. This was approached by comparing metastable-ion and CAD spectra of isomeric PAH radical cations produced by EI. As reported by Shushan et al. [13,14], abundances for metastable-ion decompositions of the [M − H]$^+$ and [M − 2H]$^+$ ions, although relatively low, can be effective at distinguishing some isomeric PAHs. Our values (see Table 1) are similar to those previously reported, and the small differences possibly are due to different source temperatures or analyzer pressures.

Unlike the relative metastable-ion abundances, the high-energy collisions and resulting fragmentations produce ions whose abundances are similar for each isomeric series of PAHs, which makes isomer differentiation nearly impossible (see Table 2). Although this lack of distinction is not unexpected [17], the results do

Table 1. Metastable-ion abundances relative to main beam of PAH radical cations

Loss	1	2	3	4	5	6	7	8	9
H·	0.36	0.53	0.30	0.39	0.36	0.79	0.35	0.30	0.40
H_2	0.07	0.16	0.13	0.10	0.08	0.14	0.11	0.14	0.08
[M − 2H]/[M − H]	0.19	0.30	0.43	0.25	0.22	0.17	0.31	0.46	0.20

set the stage for the study of bimolecular reactions of this series of PAHs.

Bimolecular Reactivity with Nucleophiles

The bimolecular reactions that occur in ionized mixtures of a PAH and pyridine or PAH and N-methylimidazole were pursued. Three classes of product ions were observed from reactions of PAHs with pyridine or N-methylimidazole. Anthracene and phenanthrene produced radical cation adducts when reacted with N-methylimidazole at CI source pressures > 0.1 torr. Collisional activation of the radical-cation adducts produced primarily $C_{14}H_{10}$ ions (presumably the PAH radical cation), but also led to some hydrogen-atom, methyl, and PAH loss. A previous study showed that naphthalene radical cations form a radical-cation adduct with N-methylimidazole and also exhibit hydrogen atom, methyl, and $C_4H_6N_2$ loss upon collisional activation [29]. Reactions of 3–9 with pyridine and N-methylimidazole did not yield radical-cation adducts. The inability to observe these adducts for the latter systems presented here probably is due to lower reactant pressures (< 0.06 torr) than those achieved with the anthracene and phenanthrene systems. Increasing source pressures with a third gas such as helium or carbon disulfide, however, was ineffective at stabilizing radical-cation adducts.

PAH/pyridine systems show reactions that give product ions 51 u higher than the mass of the PAH. The PAH/N-methylimidazole reaction systems produce a series of product ions that appear 40, 54, and 95 u above that of the PAH. The CAD spectra of these four ions proved to be ineffective in PAH isomer differentiation, because common fragment ions of nearly equal abundance were produced. All of the PAHs discussed in this article gave even-electron product ions at one mass unit lower than the sum of the reactants; these even-electron adducts are the focus of the remainder of this article. For example, in an ionized mixture of pyridine (mass 79) and benz[a]anthracene (mass 228), a product ion of m/z

Table 2. Fragment ion abundances[a] of collisionally activated PAH radical cations[b]

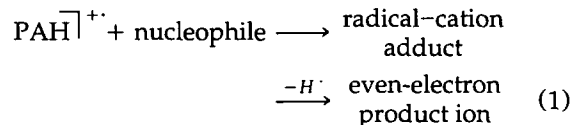| Loss	1	2	3	4	5	6	7	8	9
H	100	100	75	68	63	43	43	39	36
H_2	49	47	100	100	100	100	100	100	100
$H_2 + H$	5		8	9	9	8	12	6	7
$2H_2$			14	12	13	12	16	21	21
CH	15	14	22	10	13	10	10	7	
CH_2	6	6			7	6	5		
CH_3	10	9	35	28	27	28	24	22	20
CH_5						5		7	7
C_2H_2	7	7	6	6	5	6			
C_2H_3	15	14	5	5	9	7			
C_2H_4	8	7	14	12	14	10	12	11	10
C_2H_6								6	7
C_3H_3	9	8	9	7	6	5			5
C_3H_5			16	14	8	9	7	8	11
C_4H_4	7	7	9	6	8	8			
C_4H_5			5						
C_4H_6			5					8	8
C_5H_5			10	7	5	6			
C_6H_6			6	5					
C_7H_7	5	5							
C_8H_7	6	6							
C_8H_8	6	6							
C_9H_7	7	7							

[a] 5% minimum.
[b] Normalized to most abundant fragment ion. The precision for the relative abundances is ±10% for relative abundances greater than 10%.

306 is formed, whereas, the reaction of N-methylim-idazole (mass 82) and perylene (mass 252) gives a product ion of m/z 333 (see Figure 1). These [adduct − H]$^+$ ions will be referred to in subsequent discussion as "product ions."

The question now arises: How are these even-electron product ions formed? Previous experiments with benzene (or naphthalene) reacting with N-meth-ylimidazole revealed, through ion-selection experiments in a Fourier transform instrument, that ionization energies (IE) are the determining factor for the reaction pathways [29]. For example, neutral benzene (IE = 9.24 eV [32]) and ionized N-methylimidazole (IE = 8.66 eV [32]) react to produce an adduct ion of m/z 160, whereas for naphthalene/N-methylim-idazole, the naphthalene (IE = 8.13 eV [32]) radical cation is the reactant. The ionization energies of the PAHs investigated in this work are lower than those of the nucleophiles, which strongly suggests that the reaction pathway involves the PAH radical cation and the nucleophile neutral.

The even-electron "product ions" are likely to be formed by hydrogen-atom loss from the radical-cation adduct (see eq 1). Supporting the scheme in eq 1 are the results of an experiment in which the abundance of the putative PAH precursor radical ion was maximized with respect to other possible precursors (e.g., [PAH − H]$^+$, which is the reactant in reactions of ionized mixtures of pyrene and alkyl iodides [18]). This was accomplished by using the toluene radical cation as a charge-exchange reagent in lieu of the

high-energy electron beam. In these experiments, the relative abundances of the [adduct − H]$^+$ ions are nearly identical to those seen in the experiments in which the PAHs were ionized directly by the electron beam.

$$\overline{\text{PAH}}^{+\cdot} + \text{nucleophile} \longrightarrow \begin{array}{l} \text{radical–cation} \\ \text{adduct} \end{array}$$

$$\xrightarrow{-H\cdot} \begin{array}{l} \text{even-electron} \\ \text{product ion} \end{array} \quad (1)$$

PAH/Pyridine Reaction Products

The measurement of bimolecular reactivity between PAHs and the model nucleophile, pyridine, was pursued. Reactivity was investigated by admitting separately a PAH and pyridine to the CI source, ionizing the mixture, and observing the products. Product-ion structures were probed by collecting and comparing their CAD spectra. As shown in Figure 2, each product-ion spectrum is dominated by a cluster of ions that appear *inter alia* 78, 79, and 80 u less than that of the main beam. For example, collisional activation of the product ions from reactions of pyridine with the isomers benzo[a]pyrene, benzo[e]pyrene, and perylene all produce ions of m/z 252 (loss of C_5H_4N), m/z 251 (loss of C_5H_5N), and m/z 250 (loss of C_5H_6N). A summary of ion abundances of the PAH–pyridine
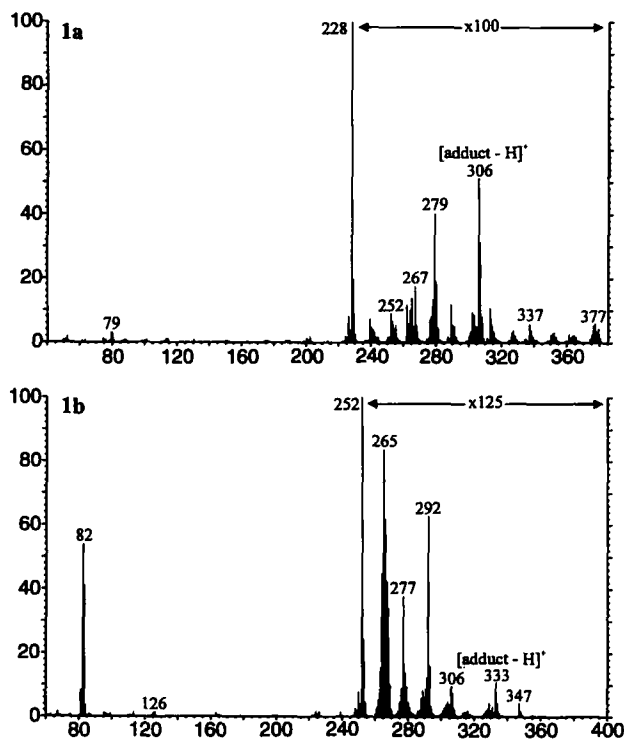

Figure 1. Low resolving power mass spectrum from an ionized mixture during high pressure CI of (a) benz[a]anthracene/pyridine and (b) perylene/N-methylimidazole.
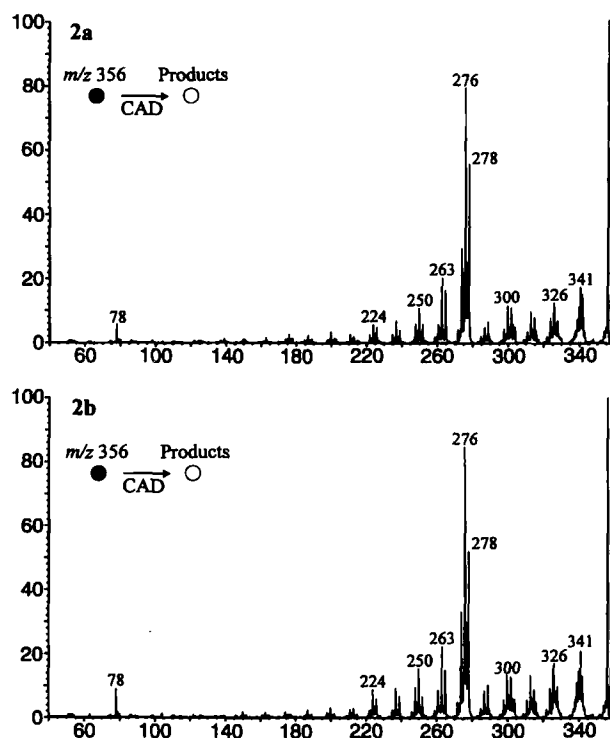

Figure 2. Collisionally induced decomposition spectra of product ions from an ionized mixture of (a) 1,2:5,6-dibenz-anthracene/pyridine and (b) 1,2:3,4-dibenzanthracene/pyridine. The spectra have been magnified by 150× for peaks below m/z 350.

product ions formed upon collisional activation shows that fragmentations and the ion abundances are similar (see Table 3). The loss of C_5H_5N (presumably neutral pyridine) is most likely the result of direct cleavage of a bond between the PAH moiety and pyridine. The loss of C_5H_4N is the result of bond breakage accompanying or following hydrogen-atom rearrangement from the pyridine moiety to the PAH and, conversely, the loss of C_5H_6N occurs by bond breakage after hydrogen rearrangement from the PAH moiety to the pyridine. Additional analysis of the data in Table 3 shows that in some instances, particularly in the case of anthracene and phenanthrene, the product ion abundances are distinct for each isomeric PAH–pyridine adduct.

PAH/N-Methylimidazole Reaction Products

To study further the inherent gas-phase reactivity of PAHs, N-methylimidazole was used as a nucleophile. This neutral was chosen because it is a volatile model of a DNA purine base. The PAH and N-methylimidazole were admitted into the CI source of the spectrometer, and the mixture was ionized to initiate reac-

tions between the two species. CAD spectra of the PAH/N-methylimidazole product ions, shown in Figures 3–6, are analogous to those of the pyridine product ions in terms of fragment-ion production, but they are much more effective at PAH isomer differentiation. The spectra show common series of high and low mass fragment ions and are dominated by three ions formed by the losses of $C_4H_5N_2$, $C_4H_6N_2$ (presumably neutral N-methylimidazole), and $C_4H_7N_2$. For example, tetracene and benz[a]anthracene react with N-methylimidazole to give a product ion of m/z 309. Upon collisional activation, the product ion undergoes $C_4H_xN_2$ losses (where x = 5, 6, or 7) to form ions of m/z 228, 227, and 226, respectively. The losses of $C_4H_xN_2$ are characteristic of each N-methylimidazole/PAH product ion, and the abundances of the three resulting fragment ions are clearly distinctive for each. The loss of $C_4H_6N_2$ is the result of direct cleavage of the bond that connects N-methylimidazole and the [PAH − H]$^+$ moiety. If the adduct has a structure in which the PAH and imidazole moieties are directly bonded, the $C_4H_5N_2$ loss is the result of hydrogen rearrangement from the N-methylimidazole moiety to the PAH followed by or in concert with bond cleavage

Table 3. Fragment-ion abundances[a] of collisionally activated PAH/pyridine ions

| Mass loss	1	2	3	4	5	6	7	8	9
1	72	79	96	100	100	100	79	100	100
2	100	100	100	84	63	81	100	85	78
3	16	16	22	16	17	14	30	18	15
4	8		11	11			12	19	21
5						7	10	8	8
14		7		8	14	15	8	7	
15	11	19	12	14	14	19	14	9	10
16		8		8	10	13	13		7
28						7			
29							9		
30	8	9		7	7	12	15	7	8
32							8		
41						17			
43							9		
53					7				
54					8	14	12		
55							7		
56					7	8	12		
67						9	7		
69						8			
78	31	12	36	26	61	70	90	27	22
79	18	31	11	8	20	10	13	10	12
80	18	24	29	22	38	55	38	38	38
81						12			
82			7		11	14	9	13	14
91	7		7	7	24	27	11	7	
93					12	12	8	9	8
105		8							
106					7	7			

[a] 7% minimum.
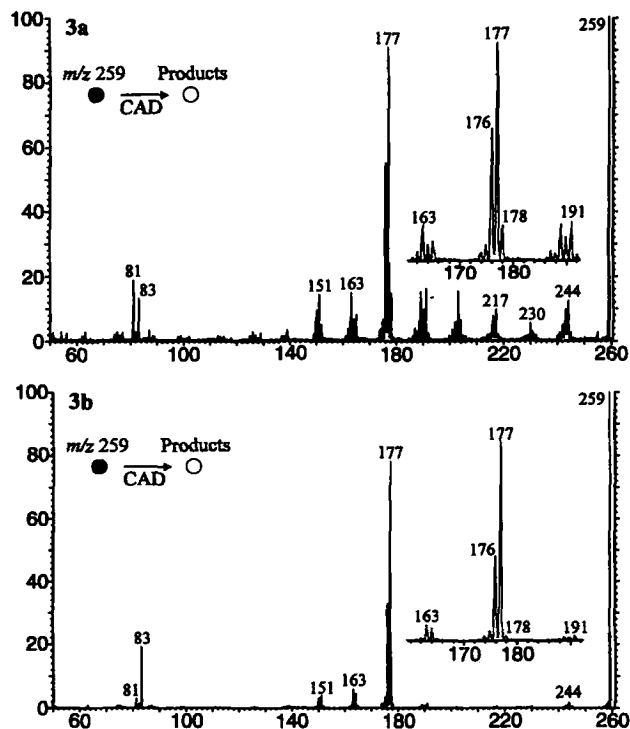
Figure 3. Collisionally induced decomposition spectra of product ions from an ionized mixture of (a) anthracene/N-methylimidazole and (b) phenanthrene/N-methylimidazole.
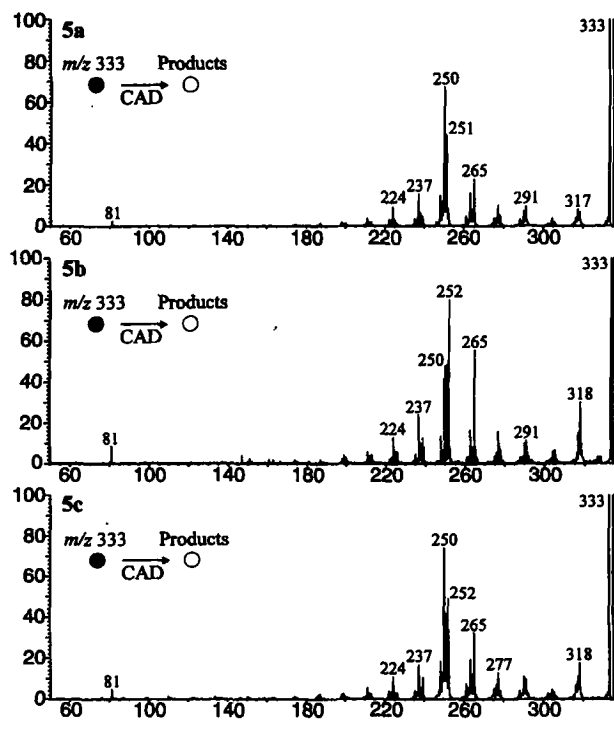

Figure 5. Collisionally induced decomposition spectra of product ions from an ionized mixture of N-methylimidazole and (a) benzo[e]pyrene, (b) benzo[a]pyrene, and (c) perylene.
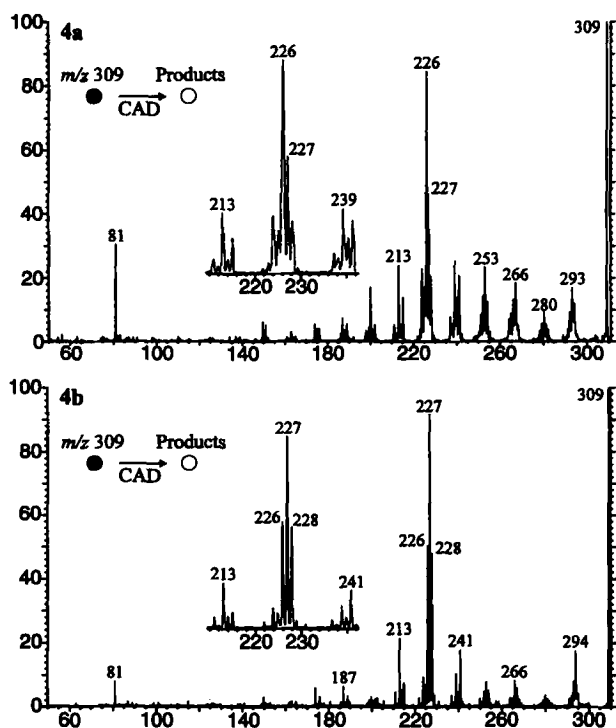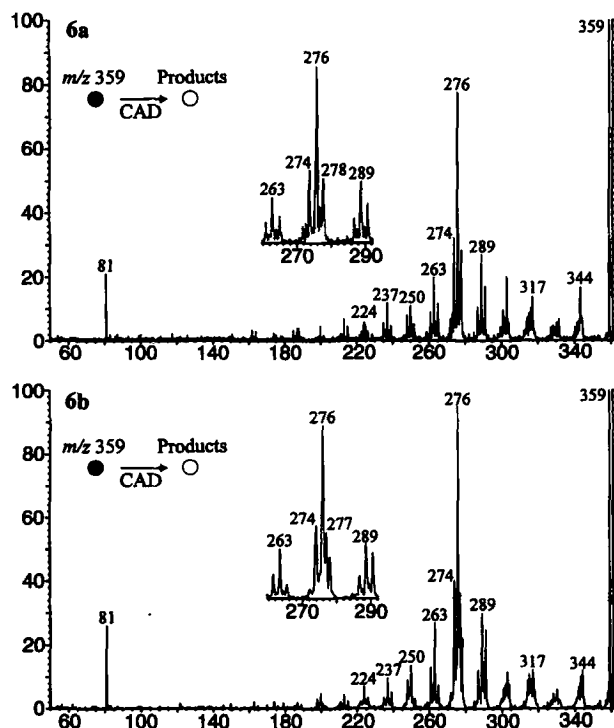

Figure 4. Collisionally induced decomposition spectra of product ions from an ionized mixture of (a) 1,2-benz[a]anthracene/N-methylimidazole and (b) tetracene/N-methylimidazole.

Figure 6. Collisionally induced decomposition spectra of product ions from an ionized mixture of N-methylimidazole and (a) 1,2:5,6-dibenzanthracene and (b) 1,2:3,4-dibenzanthracene.

to form the PAH radical cation. Conversely, $C_4H_7N_2$ loss is the result of hydrogen rearrangement from the PAH to the N-methylimidazole moiety accompanied by bond cleavage. These collisionally induced fragmentation processes occur in both the pyridine and N-methylimidazole systems, and are summarized in Scheme I.

To study further the PAH/N-methylimidazole product ions, metastable decompositions were recorded on a three-sector instrument where the product-ion resolving power is inadequate to distinguish ions separated by one mass. As shown in Figure 7, each product ion undergoes a series of metastable losses of species of 15, 27, 28, 41, 42, 56, 68, and 82 u. The losses of neutrals of 15, 27, and 41 u were noted in previous work [29] and were found to be the result of direct cleavage or cleavage in conjunction with cycloreversions of the imidazole ring. A summary of metastable-ion abundances of the PAH/N-methylimidazole systems shows that these data for PAH/N-methylimidazole product ions serve as another avenue for PAH isomer differentiation (see Table 4).

The results presented show that isomer distinction is possible under certain conditions. In the remainder of this article, we consider both qualitative and quantitative interpretations of the results. For the quantitative interpretation, the reproducibility (precision) of the spectra and a method for comparing spectra of isomers by means of a similarity index are discussed.
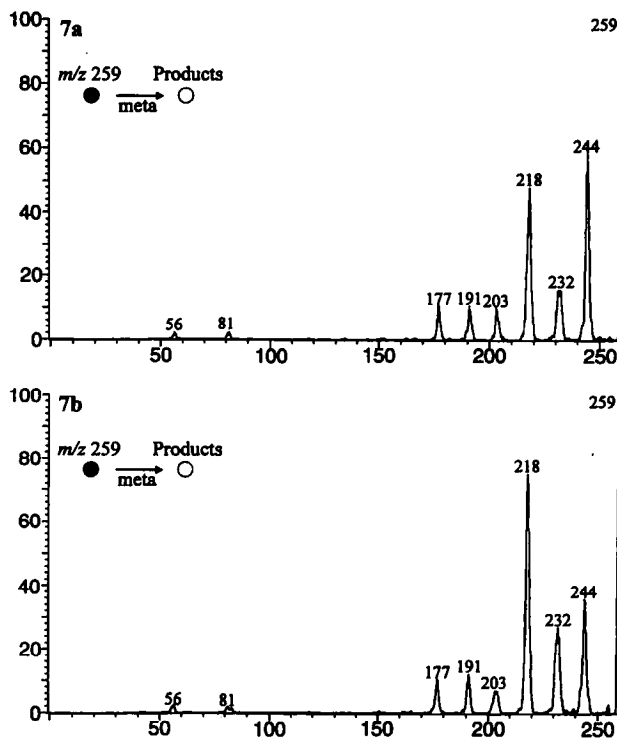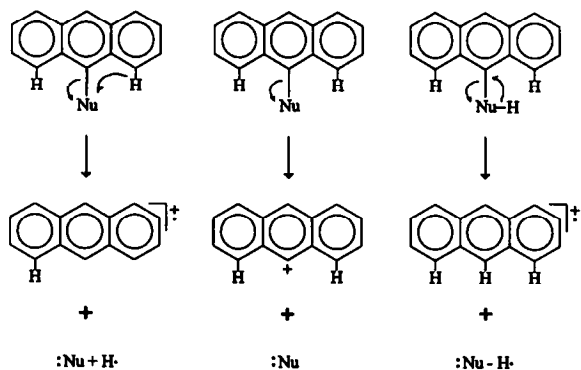

Figure 7. Metastable decomposition spectra of product ions from an ionized mixture of (a) anthracene/N-methylimidazole and (b) phenanthrene/N-methylimidazole.

Qualitative Analysis of Data

We have shown that N-methylimidazole is useful in distinguishing PAH isomers through the formation of gas-phase product ions. If the appearance of CAD and metastable-ion spectra from PAH/N-methylimidazole product ions can be predicted, analysis of these ions would be an even more useful tool for determining PAHs. At this point, there are two fundamental problems that preclude attaining this goal. The first is that the structures of the PAH/nucleophile product ions are not known. Structure determination is complicated because different PAHs have very different binding environments. PAHs such as tetracene have no "bay regions," whereas benzo[a]pyrene has one and benzo[e]pyrene has two. Second, there are various

Scheme I

Table 4. Fragment ion abundances from metastable decompositions of PAH/N-methylimidazole product ions

Loss	1	2	3	4	5	6	7	8	9
15	100	47	100	100	69	97	100	81	100
27/28[a]	27	36	17	32	18	59	15	26	31
41/42[a]	83	100	35	97	41	100	41	69	66
56	18	9	15	23	16	25	14	16	26
68	19	16	19	46	100	38	72	81	44
82	19	14	49	66	26	16	88	100	35

[a] Unresolved.

nucleophile sites on N-methylimidazole. Because there are variable reaction sites, there is a possibility to form a mixture of gas-phase product ions. The use of molecular orbital calculations of PAH/N-methylimidazole [adduct − H]$^+$ ions may yield structural information that leads to a deeper understanding of the systems and to accurate predictions of CAD and metastable-ion spectra, but these calculations were not done as part of this study. An additional problem is that even though four sets of PAH isomers were studied, these do not represent a majority of PAH isomers. Application of the techniques used in this article to a wider range of PAHs may reveal trends that are not evident at this time.

Nevertheless, attempts to understand and predict the appearance of CAD and metastable-ion spectra were made. As shown in Figures 2–6, collisional activation of PAH/nucleophile [adduct − H]$^+$ ions results in the formation of PAH radical cations. One possibility is that the relative abundance of these PAH radical cations may correlate with their enthalpies of formation (ΔH_f°), but a correlation does not exist. It was noticed, however, that the relative abundance of the fragment ions resulting from losses of $C_4H_7N_2$ (for PAH/N-methylimidazole product ions) and C_5H_6N (for PAH/pyridine product ions) tend to increase with the ΔH_f° of the PAH radical cation. Furthermore, it was noticed that the ratios of $C_4H_7N_2$:$C_4H_6N_2$ losses from PAH/N-methylimidazole product ions also tend to increase with ΔH_f° of the PAH radical cation. The existence of "bay-regions" for a PAH, if involved in the bonding of a PAH to pyridine or N-methylimidazole, also may influence the processes proposed in Scheme I. Attempts to correlate fragment ion abundances with the number of "bay regions" of a given PAH, however, were unsuccessful. A similar analysis was applied for ions formed in the metastable decomposition of PAH/N-methylimidazole adducts, but no consistent outcome for all the isomers was found. Despite these mechanistic uncertainties, the data are remarkably isomer specific, which motivates future investigations of the mechanism.

Quantitative Analysis of Data

To quantify the effectiveness of collisionally induced and metastable fragment ion abundances for PAH isomer differentiation, similarity indices (SI) were calculated by using eq 2 in which $i - i_0$ is the difference in a given ion abundance in two spectra (with i_0 as the lower abundance) and N is the number of ions used for comparison [33]:

$$SI = \sqrt{\Sigma\left(\frac{i - i_0}{i_0} \times 100\right)^2 \Big/ N} \qquad (2)$$

The SI is a quantitative measure of the similarity (or dissimilarity) of two spectra. Consecutive acquisitions of a parent ion's spectrum, which gives data that are a measure of reproducibility of spectra, should result in a low SI. CAD spectra from consecutive acquisitions of anthracene/pyridine and anthracene/N-methylimidazole product ions result in SIs of 12 and 16, respectively (see Table 5). These SI values may be viewed as standard deviations that are integrated over the entire spectrum. Often two data sets are regarded as distinct if they differ by 2 standard deviations. Therefore, for CAD spectra of product ions from isomeric PAHs with pyridine or N-methylimidazole to be effective in isomer differentiation, SI values of approximately 24 and 32 are required. Table 5 shows that CAD spectra of PAH/pyridine product ions are somewhat effective at distinguishing isomeric PAHs, particularly for 1 and 2, whereas, CAD spectra from PAH/N-methylimidazole product ions result in SI values that are quite large, and thus the spectra are much more effective at PAH isomer distinction. For PAH/pyridine fragment ions, the product ion abundances that result from collisionally induced losses of C_5H_xN ($x = 4, 5, 6$) were used. For collisionally induced fragments of PAH/N-methylimidazole product ions, the ion abundances that result from losses of $C_4H_xN_2$ ($x = 5, 6, 7$) were used. Consecutive acquisitions of metastable-ion spectra from product ions of 1 and N-methylimidazole resulted in a SI of 46. Table 5 shows that metastable-ion analysis of

Table 5. Similarity index (SI) values of collisionally and metastably produced fragment ions from isomeric [adduct − H]$^+$ ions

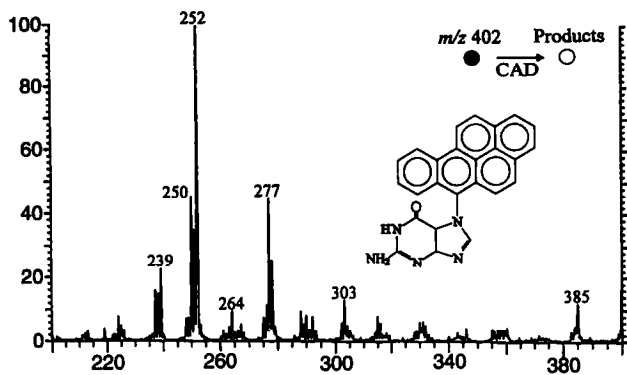| PAHs compared	Pyridine adduct (CAD)[a]	N-methylimidazole adduct (CAD)[a]	N-methylimidazole adduct (meta)[b]
1, 2	102	64	348
3, 4	36	103	117
5, 6	64	134	425
5, 7	42	101	71
6, 7	35	232	194
8, 9	17	88	81
1, 1	12	16	46

[a] $N = 3$.
[b] $N = 6$.

Figure 8. Partial collisionally induced decomposition spectrum of benzo[a]pyrene-6-N7guanine adduct.

PAH/N-methylimidazole product ions also is effective at distinguishing isomeric PAHs.

Conclusions

A goal of this work was to achieve PAH isomer distinction through reactions with model DNA bases. Product ions are shown to be formed and when collisionally activated, a rich amount of fragmentation is observed that makes isomer differentiation simple and direct. PAH/N-methylimidazole product ions are shown to produce CAD spectra that are more specific than those of PAH/pyridine product ions, possibly because N-methylimidazole has a more complex structure than that of pyridine.

A long-range goal of this work is to determine if gas-phase reactivity of PAH radical cations correlates with biological activity. As stated in the introduction, experiments by Cavalieri and co-workers have shown PAH radical cations form PAH/nucleoside adducts in solution. Tandem mass spectrometry analysis of these condensed-phase adducts yields CAD spectra that are very similar to the spectra presented here [26]. The partial CAD spectrum of the synthetic benzo[a]pyrene-6-N7-guanine adduct (Figure 8) shows a series of ions of m/z 250, 251, and 252. The relative abundances of these ions are similar to those of analogous ions of the benzo[a]pyrene/N-methylimidazole adduct shown in Figure 5b, which suggests structural similarities between the gas-phase and solution-phase adducts. Certainly the gas-phase reactivity is sufficiently selective to be used for isomer differentiation.

Acknowledgments

References

1. (a) Wilmshurst, J. R. J. Chromatog. 1965, 17, 50; (b) Lijinsky, W.; Domsky, I.; Mason, G.; Ramahi, H. Y.; Safavi, T. Anal. Chem. 1963, 35, 952; (c) Dupire, F.; Botquin, G. Anal. Chim. Acta 1958, 18, 282; (d) Dupire, F. Z. Anal. Chem. 1959, 170, 317.

2. Bjorseth, A., Ed. Handbook of Polycyclic Aromatic Hydrocarbons; Marcel Dekker: New York, 1983.

3. Lee, M. L.; Novotny, M. V.; Bartle, K. D. Analytical Chemistry of Polycyclic Aromatic Compounds; Academic: New York, 1981.

4. Vo-Dinh, T., Ed. Chemical Analysis of Polycyclic Aromatic Compounds; Wiley: New York, 1989.

5. (a) Popl, M.; Dolansky, V.; Mostecky, J. J. Chromatogr. 1974, 91, 649; (b) Popl, M.; Dolansky, V.; Mostecky, J. J. Chromatogr. 1976, 117, 117; (c) Wise, S. A.; Chesler, S. N.; Hertz, H. S.; Hilpert, L. R.; May, W. E. Anal. Chem. 1977, 49, 2306; (d) Chmielowiec, J.; George, A. E. Anal. Chem. 1980, 52, 1154; (e) Crego, A. L.; Diez-Masa, J. C.; Dabrio, M. V. Anal. Chem. 1993, 65, 1615; (f) Kibbey, C. E.; Meyerhoff, M. E. Anal. Chem. 1993, 65, 2189.

6. Weijun, J.; Changsong, L. Anal. Chem. 1993, 65, 863.

7. Nie, S.; Dadoo, R.; Zare, R. N. Anal. Chem. 1993, 65, 3571.

8. Langenfeld, J. J.; Hawthorne, S. B.; Miller, D. J.; Pawliszyn, J. Anal. Chem. 1993, 65, 338.

9. Wise, S. A.; Benner, B. A.; Chesler, S. N.; Hilpert, L. R.; Vogt, C. R.; May, W. E. Anal. Chem. 1986, 58, 3067.

10. Dobson, H. L. M.; D'Silva, A. P.; Weeks, S. J.; Fassel, V. A. Anal. Chem. 1986, 58, 2129.

11. Balasanmugam, K.; Viswanadham, S. K.; Hercules, D. M. Anal. Chem. 1986, 58, 1102.

12. Eiceman, G. A.; Vandiver, V. J. Anal. Chem. 1986, 58, 2331.

13. Shushan, B.; Boyd, R. K. Org. Mass Spectrom. 1980, 15, 445.

14. Shushan, B.; Safe, S. H.; Boyd, R. K. Anal. Chem. 1979, 51, 156.

15. (a) Bier, M. E.; Schwartz, J. C.; Schey, L. L.; Cooks, R. G. Int. J. Mass Spectrom. Ion Processes 1990, 103, 1; (b) Schey, K. L.; Cooks, R. G.; Kraft, A.; Grix, R.; Wollnik, H. Int. J. Mass Spectrom. Ion Processes 1989, 94, 1; (c) Cooks, R. G.; Ast. T.; Mabud, Md. A. Int. J. Mass Spectrom. Ion Processes 1990, 100, 209; (d) Hand, O. W.; Winger, B. E.; Cooks, R. G. Biol. Environ. Mass Spectrom. 1989, 18, 83.

16. Chen, G.; Cooks, R. G. J. Mass Spectrom. 1995, 30, 1167.

17. Pachuta, S. J.; Kenttamaa, H. I.; Sack, T. M.; Cerny, R. L.; Tomer, K. B.; Gross, M. L.; Pachuta, R. R.; Cooks, R. G. J. Am. Chem. Soc. 1988, 110, 657.

18. Nourse, B. D.; Cox, K. A.; Cooks, R. G. Org. Mass Spectrom. 1992, 27, 453.

19. (a) Simonsick, W. J., Jr.; Hites, R. A. Anal. Chem. 1984, 56, 2749; (b) Simonsick, W. J., Jr.; Hites, R. A. Anal. Chem. 1986, 58, 2114.

20. Burrows, E. P. J. Mass Spectrom. 1995, 30, 312.

21. (a) Buchanan, M. V.; Olerich, G. Org. Mass Spectrom. 1984, 19, 486; (b) Stemmler, E. A.; Buchanan, M. V. Org. Mass Spectrom. 1989, 24, 94, 705.

22. Keough, T. Anal. Chem. 1982, 54, 2540.

23. Mahle, N. H.; Cooks, R. G.; Korzeniowski, R. W. Anal. Chem. 1983, 55, 2272.

24. (a) Harvey, R. G., Ed. Polycyclic Hydrocarbons and Carcinogenesis; ACS: Washington, DC, 1985; (b) Pryor, W. A., Ed. Free Radicals in Biology; Academic: New York, 1984.

25. (a) Rogan, E. G.; Cavalieri, E. L.; Tibbels, S. R.; Cremonesi, P.; Warner, C. D.; Nagel, D. L.; Tomer, K. B.; Cerny, R. L.; Gross, M. L. J. Am. Chem. Soc. 1988, 110, 4023; (b) Cavalieri, E. L.; Rogan, E. G.; Devanesan, P. D.; Cremonesi, P.; Cerny, R. L.; Gross, M. L.; Bodell, W. J. Biochemistry 1990, 29, 4820; (c) Devanesan, P. D.; RamaKrishna, N. V. S.; Todorovic, R.; Rogan, E. G.; Cavalieri, E. L.; Jeong, H.; Jankowiak, R.; Small, G. J. J. Chem. Res. Toxicol. 1992, 5, 302; (d) RamaKrishna, N. V. S.; Cavalieri, E. L.; Rogan, E. G.; Dolnikowski, G.; Cerny, R. L.; Gross, M. L.; Jeong, H.; Jankowiak, R.; Small, G. J. J. Am. Chem. Soc. 1992, 114, 1863; (e) RamaKrishna, N. V. S.; Padmavathi, N. S.; Cavalieri, E. L.; Rogan, E. G.; Cerny, R. L.; Gross, M. L. Chem. Res. Toxicol. 1993, 6, 554.

26. RamaKrishna, N. V. S.; Gao, F.; Padmavathi, N. S.; Cavalieri, E. L.; Rogan, E. G.; Cerny, R. L.; Gross, M. L. *Chem. Res. Toxicol.* **1992**, *5*, 293.

27. Davoli, E.; Cerny, R. L.; Gross, M. L. *Adv. Mass Spectrom.* **1989**, *11A*, 268.

28. Dolnikowski, G. G.; Gross, M. L.; Cavalieri, E. L. *J. Am. Soc. Mass Spectrom.* **1991**, *2*, 256.

29. (a) Whitehill, A. B.; Mathai, G.; Gross, M. L. *J. Am. Chem. Soc.* **1996**, *118*, 853; (b) Whitehill, A. B.; Mathai, G.; Gallup, G. A.; Gross, M. L. *Polycyclic Arom. Compounds* **1994**, *5*, 87.

30. Freeman, J. A.; Johnson, J. V.; Yost, R. A.; Kuehl, D. W. *Anal. Chem.* **1994**, *66*, 1902.

31. Burinsky, D. J.; Cooks, G.; Chess, E. K.; Gross, M. L. *Anal. Chem.* **1982**, *54*, 295.

32. Lias, S. G.; Bartmess, J. E.; Liebman, J. F.; Holmes, J. L.; Levin, R. D.; Mallard, W. G. Gas-Phase Ion and Neutral Thermochemistry; *J. Phys. Chem. Ref. Data* **1988**, *17*, Suppl. 1.

33. Lay, J. O., Jr.; Gross, M. L.; Zwinselman, J. J.; Nibbering, N. M. M. *Org. Mass Spectrom.* **1983**, *18*, 16.